

Irreversibility line in $\text{YBa}_2\text{Cu}_3\text{O}_7$ samples

A comparison between experimental techniques and effect of electron irradiation

E.R. Yacoby, A. Shaulov¹ and Y. Yeshurun

Department of Physics, Bar-Ilan University, Ramat-Gan, Israel

M. Konczykowski and F. Rullier-Albenque

Laboratoire des Solides Irradiés, CEREM, Ecole Polytechnique, 91128 Palaiseau, France

Received 25 February 1992

Revised manuscript received 2 June 1992

We have investigated the irreversibility line (IRL) of a ceramic $\text{YBa}_2\text{Cu}_3\text{O}_7$ sample by probing the onset of irreversibility in four DC and AC techniques. All techniques yield a line which obeys a power law $H=A(1-T/T_c)^n$ but A and n depend on the technique. Also, the location of the peak in the AC signal obeys this power-law but it does not scale with the onset of irreversibility. We have also investigated the effect of two doses of 2.5 MeV electron irradiation on the IRL and find that after irradiation both the transition temperature T_c and the irreversibility temperature T_{irr} decrease. The decrease in T_{irr} scales with the decrease in T_c . We propose that this scaling indicates that electron-irradiation does not induce pinning centers stronger than those present in the unirradiated sample.

1. Introduction

Magnetic measurements on high-temperature superconductors (HTSC) have demonstrated that there is a broad reversible region in their field-temperature (H - T) phase diagram [1]. The onset of irreversible behavior at the “irreversibility line” [2] $T_{\text{irr}}(H)$ is described, in most experiments, by a power law $1-T/T_c=AH^n$, where A is a frequency-dependent constant and the power n (in DC measurements) is approximately $\frac{2}{3}$.

The irreversibility line (IRL) was first determined by conventional zero-field-cooled (ZFC) versus field-cooled (FC) magnetization measurements. In these measurements the irreversible temperature $T_{\text{irr}}(H)$ is the temperature below which hysteresis behavior appears; for $T>T_{\text{irr}}(H)$ the ZFC and FC branches coincide. This procedure, however, is time-consuming and the determination of $T_{\text{irr}}(H)$ de-

pends on an arbitrary criterion for the (ill-defined) onset.

Alternative procedures are based on AC magnetometry. These include the study of

- (1) loss signal [3],
- (2) harmonics of the AC response [4], and
- (3) screening efficiency to AC fields [5,6].

Experiments with the AC technique indicated that T_{irr} has a weak (logarithmic) frequency dependence [3].

In the AC techniques, the IRL is defined via the onset of nonlinear phenomena, for example, by the onset of the third harmonic signal [4]. Difficulties in determining the onset have led many researchers to use other features, e.g., the peak in the loss signal [3]. In fact, the physical meaning of the peak is controversial [4,7–10] and its location depends on the sample dimensions. Nevertheless, the temperature and field dependence of the peak have served as an approximate indicator to the IRL.

In the present article we compare IRLs obtained from DC and AC data for the same samples. For the AC data we explore the temperature and field de-

¹ Permanent address: Philips Laboratories, North American Philips Corporation, Briarcliff Manor, NY 10510, USA.

pendence of both features, peaks and onsets, with the explicit intention of testing the quality and reliability of both approaches.

A second goal of this article is to verify an intriguing “scaling” feature which was implied by our preliminary study of the IRL in an electron irradiated $\text{YBa}_2\text{Cu}_3\text{O}_7$ (YBCO) ceramic sample [11]. After irradiation, we observed a small reduction of both T_c and $T_{\text{irr}}(H)$. However, the reduction in T_{irr} scaled with the reduction in T_c . Our work was motivated by conflicting results reported in the literature, for the effect of irradiation on the IRL. Work done [11,13] on $\text{Bi}_2\text{Sr}_2\text{CaCu}_2\text{O}_8$ with neutrons and other ions indicated enhancement of the pinning centers accompanied by a shift of T_{irr} to higher temperatures and fields. On the other hand, Civale et al. [14] found that the IRL of YBCO is largely independent of the defect induced by proton irradiation, even at defect levels which enhanced the irreversible magnetization by more than an order of magnitude. More recently, two groups reported a shift of the IRL after irradiation with high-energy heavy ions: Konczykowski et al. [15] reported a dramatic shift of the IRL, after lead irradiation, to higher reduced temperature; that shift is accompanied by a change of the slope sign, and Civale et al. [16] reported a shift in the IRL after irradiation with Sn ions.

Our observation of scaled T_{irr} suggests that some of the observed changes in the IRL are directly related to deterioration of the superconducting phase. The purpose of this work is to further test this implication by measuring the IRL for a sample which was exposed to a much higher level of irradiation.

This article is organized in the following way. In section 2, we provide details of the various experimental techniques used in this work. In section 3.1 we compare the IRLs obtained by four different techniques for the same sample. In section 3.2 we deal with the effect of electron irradiation on the IRL. Finally, we conclude in section 4 by summarizing the implication of our results on future measurements.

2. Experimental procedure

For determining the IRL, we used four experimental techniques:

(1) the first class consisted of conventional ZFC

versus FC magnetic measurements. Those measurements were made on a commercial SHE SQUID. The ZFC branch of the magnetization M was measured during heating of the sample, after cooling it to low temperature in zero field, and then applying a field H . With the same field still on, we cooled the sample to the same temperature and measured the FC branch, again during heating.

(2) AC screening-efficiency measurements were made by using two miniature coils – driving and detective coils – which were glued on opposite surfaces of the sample. The measured quantity was the mutual inductance between the coils, as a function of temperature, under a static magnetic field. The experimental data is presented [5] in the form of the complex transmittivity $t = T' + iT'' = (M - M_2) / (M_N - M_s)$, where M_s and M_N denote mutual inductance in the superconducting (far below T_c) and in the normal state, respectively. The measurements were taken under ZFC and FC conditions and the IRL was determined from the split of ZFC/FC curves of T' .

(3) Then, we performed measurements of the imaginary component, T'' , of the transmittivity, under ZFC conditions. The experimental procedure is as described in the second technique. The IRL is defined via the onset of this signal. We also describe the temperature and field dependence of the peak of T'' .

(4) To conclude, we mention measurements of the third harmonic in the AC response. The circuit consists of a primary coil coaxial with a pair of balanced coils, one of which contains the sample. A small sinusoidal field, superimposed on a steady DC field, induces small oscillations in the magnetization of the sample, and thus in the secondary coil which contains the sample. The output voltage of this coil is fed into a spectrum analyzer. Odd harmonics of the original signal are observed when the magnetization is not linear with the field, i.e., in the irreversible regime. We defined the onset of the third harmonic as T_{irr} for the applied field H .

We used three sintered $\text{YBa}_2\text{Cu}_3\text{O}_7$ samples with transition temperature of $T_c = 87$ K – determined by magnetic measurements – and dimensions $4 \times 4 \times 0.1$ mm³. We refer to the three samples as #1, #2 and #3, respectively. Sample #1 was used for the measurements of the IRL by the four techniques

(section 3.1). This sample also served as an unirradiated reference. Samples #2 and #3 were irradiated at 20 K by 2.5 MeV electrons produced by a Van de Graaff accelerator. Sample #2 was exposed to an electron dose of 2.54×10^{18} electrons/cm², and sample #3 to a dose of 5.45×10^{18} electrons/cm². The electrons produced damage consisting of homogeneously distributed isolated Frenkel pairs on all sublattices of YBCO [17]. However, the agglomeration of small defect clusters is expected when the sample is warmed to room temperature for transfer to the cryostat for measurements, and the total damage after annealing at room temperature is estimated [17] to be 0.0005 dpa (displacement per atom) and 0.001 dpa for samples #2 and #3, respectively.

3. Results and discussion

3.1. Comparison between different techniques

All four techniques yield an IRL which obeys a power law $H=A[1-T_{\text{irr}}/T_c]^n$ with some variations in the constant A , and in the exponent n . The field-dependence of the location of the peak obeys a similar power law. Table 1 summarizes these parameters.

In the following, we present raw data for the four techniques and compare the IRLs obtained from each of these techniques. We first compare the IRLs obtained by the two AC techniques; we then compare these results with the IRLs obtained by the other technique.

In fig. 1 we present raw data of the third harmonic signal V_3 as a function of temperature. The measurement frequency was 20 kHz, the AC field am-

plitude was 50 mOe and a DC field of 265 Oe was applied. The arrows in the figure show the onset and the peak of the signal.

Figure 2 shows raw data of the imaginary part of the transmittivity T'' as a function of temperature. The measurement frequency was 11.7 kHz, the AC field amplitude was 28 mOe and the DC field of 250 Oe was applied. Again the arrows show the onset and the peak of the signal.

In fig. 3 we present the field-temperature dependence of the peaks of T'' and of V_3 for various frequencies. For comparison, we also add the IRL obtained from the onset of V_3 . In this figure the amplitude of the AC field for T'' data is 28 mOe and the frequencies are 117 kHz, 11.7 kHz and 1.17 kHz while the V_3 measurement was carried out with amplitude of 50 mOe and a frequency of 20 kHz. The figure demonstrates that all lines obey a power law. The lines obtained from the peaks in the AC signals have very similar powers (see table 1). A similar dependence of the prefactor on frequency was observed in previous works [3,11]. The prefactor obtained from the third harmonic signal differs from the prefactors obtained from T'' . If we assume that the prefactor depends only on frequency, the IRL obtained from the third harmonic has to be located between the line of T'' in 117 kHz and the T'' line in 11.7 kHz near the latter. However, from fig. 3 it is apparent that the V_3 line is shifted beyond the first one. The line obtained from the onset of the third harmonic differs from the lines obtained from the peaks of the AC signal, both in the power n and in the prefactor.

In order to explain the shift of the lines obtained from the peaks of V_3 , relative to the peaks of T'' , we

Table 1
Summary of the IRL parameters obtained from the fit to a power law for YBa₂Cu₃O₇ sample #1

Technique	A ($\times 10^7$ Oe ⁻ⁿ)	n	Frequency (kHz)
V_3 peak	1.6	3.0	20
T'' peak	2.5	3.1	117
T'' peak	4.7	3.1	11.7
T'' peak	21.4	3.2	1.17
V_3 onset	1.2	2.5	20
T'' onset	1.2	2.5	11.7, 1.17
M ZFC/FC split	1.9×10^{-3}	1.3	
T' ZFC/FC split	6.2×10^{-2}	2.3 ^{a)}	

^{a)} Data taken from sample #3.

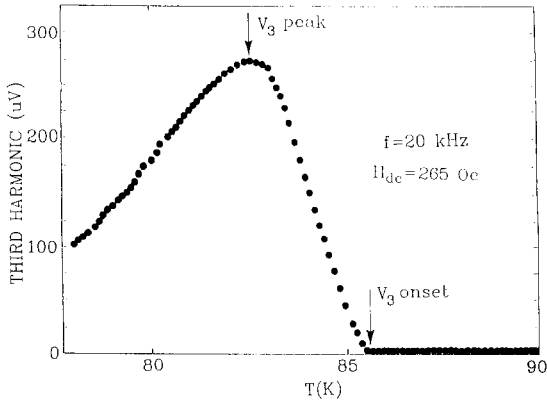


Fig. 1. Temperature dependence of the third harmonic signal in DC field of 265 Oe, $H_{AC}=50$ mOe and $f=20$ kHz. Arrows indicate onset and peak of the signal.

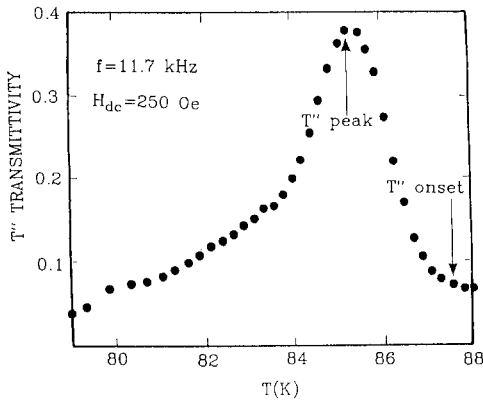


Fig. 2. Temperature dependence of the imaginary components of transmittivity in a DC field of 250 Oe, $H_{AC}=18$ mOe and $f=11.7$ kHz. Arrows indicate onset and peak of the signal.

recall that for the third harmonic signal at the peak $J_c D/H_{AC} = (0.58 c/2\pi)$ [18], whereas for the imaginary part of the transmittivity $J_c D/H_{AC} = (0.25 c/2\pi)H_{AC}$ [5], where D is the sample thickness and c is the velocity of light. (Throughout this paper J_c is the supercurrent at the time-window of the experiment; at low temperatures and low fields, in the absence of relaxations, it is the critical current.) From these equations it is apparent that the third harmonic signal will reach the peak in a higher critical current than the T'' signal, i.e., lower temperature. Another factor that will shift the peak to lower temperature is the amplitude of the AC fields in our measurements: 50 mOe and 28 mOe for the mea-

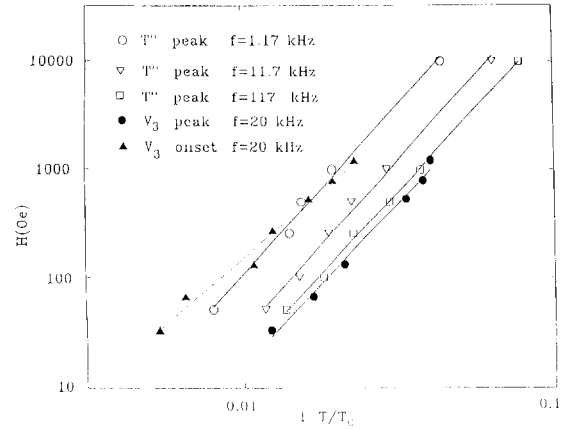


Fig. 3. The irreversibility line (IRL) and the location of the peaks for sample #1. (a) The peak in the imaginary component of the transmittivity for $H_{AC}=28$ mOe and for the indicated frequencies. (b) Third harmonic signal with $f=20$ kHz and $H_{AC}=50$ mOe. Full circles: signal peaks, full triangles: onset.

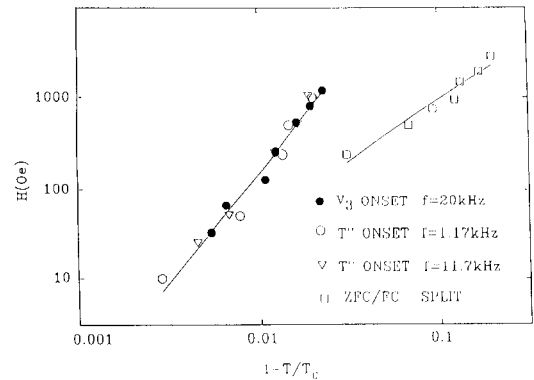


Fig. 4. The IRL for sample #1. (a) The IRL determined by the onset in the third harmonic signal with $f=20$ kHz, full circles. (b) The IRL determined by the onset in the imaginary component of transmittivity: open circles $f=1.17$ kHz and open triangles $f=11.7$ kHz. (c) The IRL determined by DC technique from the temperature above which the ZFC and FC magnetization curves coincide within 0.5% of the measured signal: open squares.

surements of V_3 and T'' , respectively. This discussion gives a quantitative explanation why the line obtained from the peak of the V_3 signal shifted to lower temperatures, i.e., to higher $1-T/T_c$ values. The difference in the conditions of the peaks raises the question of whether the peaks in these two signals in fact describe the same phenomena.

In fig. 4 we present the IRL obtained from the onset of the third harmonic signal in a frequency of

20 kHz and from the onset of the T'' signal in the frequencies 11.7 kHz and 1.17 kHz. All of the three lines fit the power law with the same master curve with $n=2.46$ and $A=1.23 \times 10^7$. Likewise, we present in this figure the IRL obtained from the split of the DC ZFC and FC magnetization branches. Typical data of DC magnetization in a field of 250 Oe is shown in fig. 5. This line obeys the power law with $n=1.30$ and a prefactor $A=1.90 \times 10^4$. From this figure one can conclude that the dependence of the IRL obtained via the onsets of T'' on frequency is much weaker than the frequency dependence of the lines obtained from the peaks of the same signal. This weak frequency dependence was observed also in the third harmonic measurements in the frequencies 60 kHz and 20 kHz. The IRL obtained from V_3 in a frequency of 20 kHz coincide with the two IRL obtained from the onset of T'' in agreement with the conclusion that the IRL obtained via the onsets has a weaker dependence on frequency.

The DC IRL of fig. 4 has a power of $n=1.30$ in agreement with other works [19]. The location of this line in relation to the AC lines can be understood via a weak dependence on frequency. The difference in frequency is approximately 6 orders of magnitude (the SQUID frequency is about 0.03 Hz).

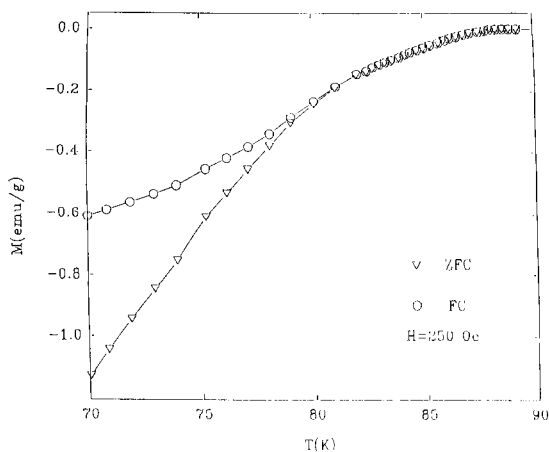


Fig. 5. Temperature dependence of DC magnetization in a field of 250 Oe. Open triangles denote the magnetization after being zero field cooled and open circles the magnetization after field cooled.

This difference in frequency can explain the location of the DC IRL. From fig. 4 one can possibly learn that the exponent n is also dependent on frequency.

Typical data of ZFC versus FC branches of the transmittivity are presented in fig. 6. Usually, AC techniques are not sensitive to the magnetic “history” of the sample. Here, however, we take advantage of the interplay between intragrain and intergrain magnetization. In a relatively narrow range of DC fields (100 Oe to 500 Oe) the response of the intragrain magnetization to the AC field is affected by the intergrain magnetization [5,6,20,21] and it thus depends on the magnetic history. In the low-field limit the intergrain currents mask the grains. In the high field limit, the intragrain currents are attenuated to such a level that history effects cannot be detected. From the data obtained from this method we conclude that the split is independent of the measuring frequency and of the AC field amplitude. The $T_{irr}(H)$ points we obtained using this method located between the line obtained by the DC technique and the lines obtained from the AC technique with the onset definition (see table 1). It seems that this line reflects DC IRL properties, and it differs from the line obtained from DC magnetization in the rate of data collection, i.e., the actual frequency is greater than the actual DC magnetization frequency.

In summary of this part of the paper, we have determined experimental lines in the H - T phase dia-

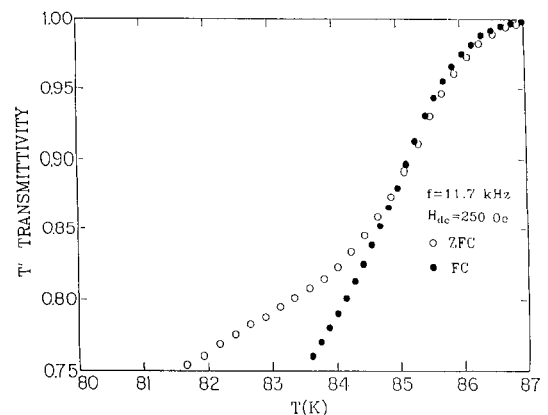


Fig. 6. The split of ZFC (open circles) and FC (full circles) branches of the AC screening efficiency in a field of 250 Oe. $H_{AC}=180$ mOe and $f=11.7$ kHz.

gram of an YBCO ceramic sample, all of which obey a power law in T/T_c . Some of these lines are directly related to the IRL. These are the lines obtained from the onset of irreversibility in the DC experiments and in the AC response. Results obtained from the onset of T'' and third harmonic show very similar IRLs with a weak frequency dependence. The IRL obtained via the split in the ZFC/FC magnetization differs from the lines obtained by AC techniques, perhaps reflecting the frequency dependence of the IRL. The equivalent lines in the H - T phase diagram which were determined from the peaks in the AC response also obey a power law, and describe only roughly the qualitative behavior of the IRLs determined from the onset of irreversibility. We also observed a stronger frequency dependence of the peaks. We may thus conclude that the conditions which determine these peaks are apparently very different from those which define the onset of irreversibility.

3.2. Irradiation effects

Figure 7 presents the IRL which was obtained from the onset of the third harmonic signal for all three samples (the reference one (#1) and the two damaged samples (0.0005 dpa and 0.001 dpa)). From this figure one can see that both T_c and $T_{irr}(H)$ for sample #2 show a small reduction (< 1 K) as a result of the irradiation. For sample #3 T_c is reduced by 4 K and a significant reduction of $T_{irr}(H)$ is also

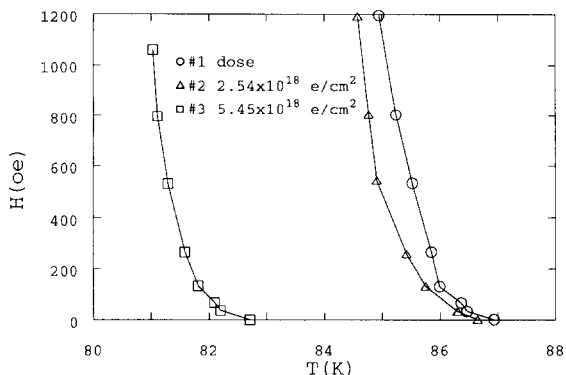


Fig. 7. The IRL determined by the onset in the third harmonic signal before and after irradiation in the form of $H(T)$. Open circles denote sample #1 (as grown), open triangles sample #2 (dose 2.54×10^{18} electrons/cm²) and open squares sample #3 5.45×10^{18} electrons/cm².

observed. However, fig. 8 demonstrates that the three IRLs presented in fig. 7 coincide nicely if the temperature axis is replaced by the reduced temperature $1 - T/T_c$. The solid line in this figure describes a power law with $n=2.46$ and a prefactor $A=1.2 \times 10^7$.

Figure 9 presents the lines obtained via the peak in the T'' signal at a frequency of 11.7 kHz for all three samples. There is a small effect of irradiation on the prefactor, mainly on sample #3 (see table 2).

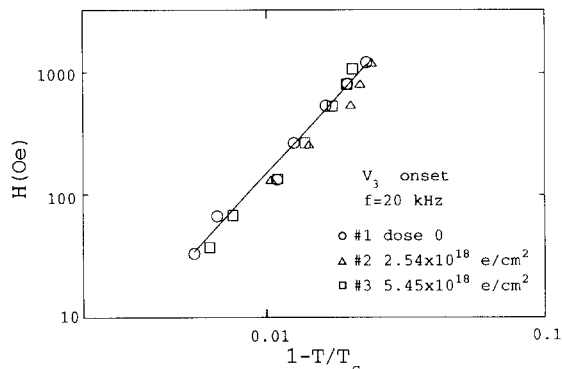


Fig. 8. The IRL determined by the onset in the third harmonic signal before and after irradiation in the form of $\text{Log}(H)$ as a function of $\text{Log}(1 - T/T_c)$. Open circles denote sample #1 (as grown), open triangles sample #2 (dose 2.54×10^{18} electrons/cm²) and open squares sample #3 (dose 5.45×10^{18} electrons/cm²).

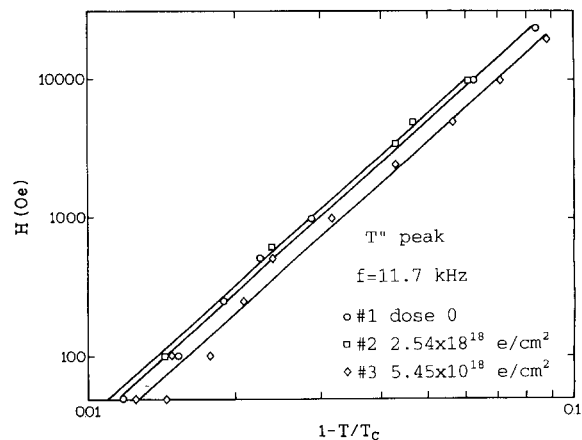


Fig. 9. $\text{Log}(H)$ vs. $\text{Log}(1 - T/T_c)$ of the peak in the imaginary component of the transmittivity before and after irradiation; $f=11.7$ kHz. Open circles denote sample #1 (as grown), open squares sample #3 (dose 2.54×10^{18} electrons/cm²) and open diamonds sample #3 (dose 5.45×10^{18} electrons/cm²).

Table 2

Summary of the IRL parameters before and after irradiation. The parameter A is in units of Oe^{-n}

Technique	Sample #1		Sample #2		Sample #3		Frequency (kHz)
	$A(10^7)$	n	$A(10^7)$	n	$A(10^7)$	n	
V_3 onset	1.2	2.5	1.2	2.5	1.2	2.5	20
T'' peak	4.7	3.1	5.4	3.1	3.3	3.1	11.7
T'' onset ^{a)}	21.3	3.0	–	–	21.3	3.0	11.7

^{a)} The difference of the fit parameters between table 1 and table 2 is because the high fields are taken into account in the fit of table 2.

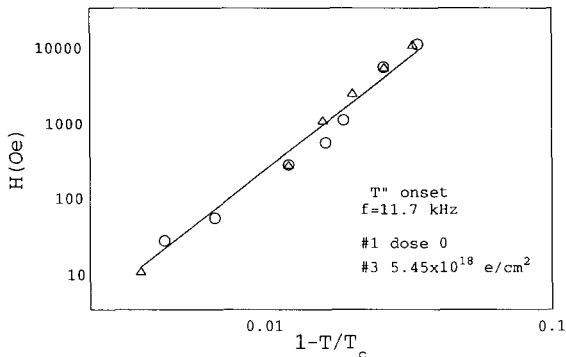


Fig. 10. The IRL determined by the onset in the imaginary component of transmittivity before and after irradiation in the form of $\text{Log}(H)$ as a function of $\text{Log}(1 - T/T_c)$, $f = 11.7$ kHz. Open circles denote sample #1 (as grown) and open triangles sample #3 (dose 5.45×10^{18} electrons/cm²).

Figure 10 presents the IRLs obtained from the onset of the T'' signals at a frequency of 11.7 kHz for samples #1 and #3. In contrast with the results presented in fig. 9, the lines presented in fig. 10 do not show any significant effect of the irradiation (in the reduced temperature axis) and both curves can fit a master line with $n=3$ and $A=2.13 \times 10^8$.

The most intriguing observation of this work is the simple scaling feature of the IRL with $t = T_{\text{irr}}/T_c$, before and after irradiation. Following arguments similar to that given in ref. [3] this feature may have an explanation in the context of bulk pinning. We express the pinning energy U_0 as $p(H_c^2/8\pi)a_0^2\xi$ where a_0 is the Abrikosov lattice constant, ξ is the coherence length, H_c is the thermodynamic field and $p \leq 1$ is related to the efficiency of the relevant pinning center [22]. Taking $a_0^2 = \phi_0/H$, and the temperature dependence of H_c and ξ , one finds [2,3] that U_0 is proportional to $p(1-t)^{3/2}/H$. At the irreversibility

line $U_0 = kT_c \ln(f_0/f)$ where f_0 is a characteristic attempt frequency and f is the measurement frequency [3]. We thus find that at the IRL the field H is proportional to $p(1-t)^{3/2}$. In other words, the IRL is predicted to scale with the reduced temperature t provided that the ‘‘pinning efficiency’’ p is not affected by irradiation. The observed scaling thus implies that near T_c the irradiation did *not* introduce new effective pinning centers.

From hysteresis loops at low temperatures (4 K and 17 K) before and after irradiation and by using the Bean model [7,26], we find that, as a result of the electron irradiation, the intracritical current J_c increased by a factor of 2. Further indirect evidence for the increase in J_c is deduced from the lowering of the height of the peak in the third harmonic signal, measured as a function of temperature. This result, an increase in J_c without a change in T_{irr}/T_c , is in agreement with the result reported by Civale et al. [14] after proton irradiation. The size of defects created by protons is 30 Å while the size of defects created by an electron is even smaller [11]. Thus, the fact that these two experiments did not show any significant change in the IRL, indicates that to affect the IRL we need to create damage on a much larger scale.

However, the increase in defect concentration in the samples broadens the width of the hysteresis loops; thus we argue [15] that for broader width of hysteresis loops, increase of defect concentration is enough, while to affect the IRL (i.e., to increase the irreversible regime), defects with pinning potentials larger than the ones existing in the sample before irradiation need to be created.

Acknowledgements

It is a pleasure to thank H. Pascard for providing the ceramic samples. The authors thank L. Klein for suggestions and helpful discussions. The work in Israel is partially supported by the Fund for Research and Development administered by the Ministry of Science and Technology.

References

- [1] K.A. Muller, M. Takashige and J.G. Bednorz, *Phys. Rev. Lett.* 58 (1987) 408.
- [2] Y. Yeshurun and A.P. Malozemoff, *Phys. Rev. Lett.* 60 (1988) 2202.
- [3] A.P. Malozemoff, T.K. Worthington, Y. Yeshurun, F. Holtzberg and P.H. Kes, *Phys. Rev. B* 38 (1988) 7203.
- [4] A. Shaulov and D. Dorman, *Appl. Phys. Lett.* 53 (1988) 2680.
- [5] J. Gilchrist and M. Konczykowski, *Physica C* 168 (1990) 123.
- [6] M. Konczykowski and J. Gilchrist, *Physica C* 168 (1990) 131.
- [7] C.P. Bean, *Rev. Mod. Phys.* 36 (1964) 31.
- [8] V.B. Geshkenbein, V.M. Vinokur and R. Fehrenbacher, *Phys. Rev. B* 43 (1991) 3748.
- [9] E.H. Brandt, *Physica C* 185–189 (1991) 270; *ibid.*, *Int. J. Mod. Phys. B* 5 (1991) 751.
- [10] L. Krusin-Elbaum, L. Civale, F. Holtzberg, A.P. Malozemoff and C. Field, *Phys. Rev. Lett.* 67 (1991) 3156.
- [11] M. Konczykowski, F. Rullier-Albenque, Y. Yeshurun, E.R. Yacoby, A. Shaulov and J. Gilchrist, *Supercond. Sci. Technol.* 4 (1991) S445.
- [12] A. Gupta, P. Esquinazi, H.F. Braun, H.-W. Neumuller, G. Ries, W. Schmidt and W. Gerhauser, *J. Phys. C* 170 (1990) 95.
- [13] W. Gerhauser, H.-W. Neumuller, W. Schmidt, G. Ries, G. Saemann-Ischenko, H. Gerstenberg and F.-M. Sauerzopf, *Physica C* 185–189 (1991) 2273.
- [14] L. Civale, A.D. Marwick, M.W. McElfresh, T.K. Worthington, F.H. Holtzberg, J.R. Thompson and M.A. Kirk, *Phys. Rev. Lett.* 65 (1990) 1164.
- [15] M. Konczykowski, F. Rullier-Albenque, E.R. Yacoby, A. Shaulov, Y. Yeshurun and P. Lejay, *Phys. Rev. B* 44 (1991) 7167.
- [16] L. Civale, A.D. Marwick, T.K. Worthington, M.A. Kirk, J.R. Clem and F. Holtzberg, *Phys. Rev. Lett.* 67 (1991) 648.
- [17] H. Vichery, F. Rullier-Albenque, H. Pascard, M. Konczykowski, R. Korman and D. Favrot, *Physica C* 159 (1989) 689.
- [18] L. Ji, R.H. Sohn, G.C. Spalding, C.J. Lobb and M. Tinkham, *Phys. Rev. B* 40 (1989) 10936.
- [19] See, for example, ref. [2].
- [20] J.E. Evetts and B.A. Glowacki, *Cryogenics* 28 (1988) 641.
- [21] A. Shaulov, Y. Yeshurun, S. Shatz, R. Hareuveni, Y. Wolfus and S. Reich, *Phys. Rev. B* 43 (1991) 3760.
- [22] P.W. Anderson, *Phys. Rev. Lett.* 9 (1962) 309; Y.B. Kim, *Rev. Mod. Phys.* 36 (1964) 39; A.M. Campbell and J.E. Evetts, *Adv. Phys.* 21 (1972) 199.
- [23] E.H. Brandt, *J. Low Temp. Phys.* 28 (1977) 291.
- [24] A. Houghton, R.A. Pelcovits and A. Sudbo, *Phys. Rev. B* 40 (1989) 6763.
- [25] E.H. Brandt, *Phys. Rev. Lett.* 63 (1989) 1106.
- [26] M. Daumling and D.C. Larbalestier, *Phys. Rev. B* 40 (1989) 9350.